Band-to-band photoluminescence in SrTiO₃

Yasuhiro Yamada[1] and Yoshihiko Kanemitsu[1,2,*]

[1]*Institute for Chemical Research, Kyoto University, Uji, Kyoto 611-0011, Japan*
[2]*Photonics and Electronics Science and Engineering Center, Kyoto University, Kyoto 615-8510, Japan*
(Received 9 July 2010; revised manuscript received 16 August 2010; published 17 September 2010)

We report the observation of band-edge photoluminescence (PL) in highly photoexcited SrTiO₃ and electron-doped SrTiO₃ at low temperatures. Two band-edge PL peaks coincide with the low- and high-temperature onsets of optical absorption. This clearly shows that band-edge PL peaks correspond to indirect band-to-band radiative recombination involving phonon emission and absorption processes and allows a determination of the band gap. The PL peaks redshift with increasing carrier density, indicating band-gap shrinkage. The temperature dependence of the band-edge PL and optical absorption spectra are also discussed in conjunction with phonon-assisted optical transitions.

Strontium titanate (SrTiO₃) is one of the most promising oxides for applications in electronics and optoelectronics. Because single-crystalline SrTiO₃ is an excellent platform material for the epitaxial growth of oxide thin films,[1,2] oxide-based electronic devices can be integrated on SrTiO₃ crystals. Moreover, SrTiO₃ itself has intriguing and multifunctional electronic properties. With low levels of electron doping, SrTiO₃ undergoes transitions from an insulator to a semiconductor, metal, and even superconductor at low temperatures.[3–6] The high mobility of charge carriers in SrTiO₃ and their unique characteristics have recently attracted considerable attention in the fields of epitaxial thin film,[7] two-dimensional heterointerfaces,[8–11] and field-induced superconducting surfaces.[12] Despite extensive research on the electronic structure and electrical properties of SrTiO₃ bulk crystals and heterostructures, the band-edge structure of SrTiO₃, which is most important in determining the electronic properties, still remains unclear, and an understanding thereof has been a long-standing difficulty in the science of oxide electronics.

In studying the band-edge electronic structure of materials, photoluminescence (PL) spectroscopy is one of the most powerful tools. Much effort has been devoted to the understanding of the PL properties of SrTiO₃. It has been reported that a broad green PL band appears around 2.5 eV at low temperatures.[13–15] In addition, a blue PL band was recently observed at around 2.9 eV in both electron-doped SrTiO₃ (Refs. [16–18]) and undoped SrTiO₃ under intense photoexcitation.[17–20] However, the green and blue PL bands have a large Stokes shift, indicating that the initial states are far from the band edge, and so far, band-edge PL in SrTiO₃ has not been reported.

In this Rapid Communication, we report the observation of band-edge PL in SrTiO₃. Two band-edge PL peaks were observed in SrTiO₃ under high-density photoexcitation. The PL peaks coincide with the low- and high-temperature onsets of the optical absorption. Based on this result, we conclude that the two PL peaks correspond to phonon-assisted radiative recombination of photoexcited electrons and holes. Similar PL peaks were observed in electron-doped SrTiO₃ under continuous-wave (cw) photoexcitation. We discuss the temperature dependence of the PL and optical absorption

spectra in conjunction with phonon-assisted band-to-band transitions.

We used undoped SrTiO₃ single crystals and three types of electron-doped SrTiO₃ single crystals: SrTi$_{1-x}$Nb$_x$O₃ ($x=0.0005$, 0.001, 0.004, 0.01, and 0.02), Sr$_{1-y}$La$_y$TiO₃ ($y=0.001$ and 0.01) (Furuuchi Chemical Co.), and Ar⁺-irradiated SrTiO₃ (acceleration voltage: 300 V and Ar gas flow: 3 ml min⁻¹). All samples were 0.5 mm thick. The undoped samples were annealed under oxygen flow for 24 h at 700 K to reduce oxygen vacancies. The PL spectra of undoped SrTiO₃ were obtained by means of time-resolved PL measurement with a time resolution of 40 ps using a streak camera and a monochromator. The light source for photoexcitation was an optical parametric amplifier system based on a regenerative amplified mode-locked Ti:sapphire laser with a pulse duration of 150 fs and a repetition rate of 1 kHz. The photon energy was 3.54 eV. The spectral resolution of this setup was ∼2 meV at 3.2 eV. The laser-spot size on the sample surface was 90 μm, which was measured using the knife-edge method. The PL measurement in electron-doped SrTiO₃ was performed under cw photoexcitation (using a He-Cd laser, photon energy: 3.82 eV) with a monochromator and a charge-coupled device camera. The laser spot size was 400 μm. The spectral resolution of the setup used with the doped samples was ∼1 meV at 3.2 eV.

The inset of Fig. 1(a) shows time-integrated and time-gated (0–8 ns) PL spectra of SrTiO₃ under high-density excitation of 5 mJ/cm² at 8 K. The time-integrated PL spectrum shows a single green PL band at around 2.5 eV. This highly efficient and long-lived PL band probably results from defects or unintentional impurities.[13,14] Because of its high efficiency and long lifetime at low temperatures, the green PL becomes dominant in time-integrated PL spectrum. On the other hand, the time-gated PL spectrum shows two PL bands: a broad blue PL band at around 2.9 eV and a sharp peak near the band-gap energy. Note that the blue PL and band-edge PL bands are observed only under intense photoexcitation using a pulsed laser.

Figure 1(a) shows an enlarged view of the time-gated (0–8 ns) PL spectrum near the band-gap energy. We observed two PL peaks at approximately 3.22 and 3.27 eV. The band-edge PL peaks are asymmetric and have longer tails on the low-energy side. The spectral widths of the two peaks have
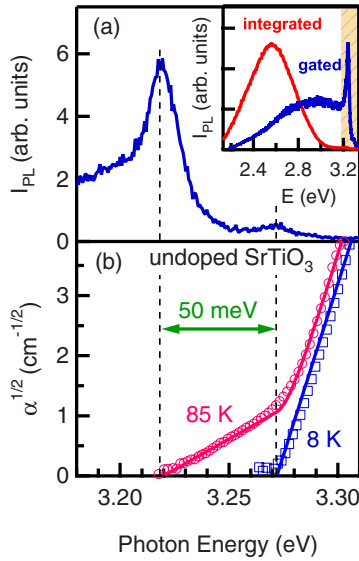
FIG. 1. (Color online) (a) Time-gated (0–8 ns) PL spectrum of SrTiO$_3$ under excitation of 5 mJ/cm^2 at 8 K. The inset shows the time-gated (0–8 ns) and time-integrated PL spectra of SrTiO$_3$ between photon energies in the range 2.15–3.3 eV at 8 K. (b) The square root of the absorption coefficient, α, at 8 and 85 K is also plotted. The solid curves are the theoretical ones for 8 and 85 K with the phonon energy of 25 meV.

almost the same value (FWHM=15 meV). The square root of the optical absorption coefficient, α, at 8 and 85 K are shown in Fig. 1(b). The fact that $\alpha^{1/2}$ varies linearly with energy is evidence that SrTiO$_3$ is an indirect-gap semiconductor. Furthermore, no excitons are formed because of the large dielectric constant. The energy separation between the low- and high-temperature onsets of the optical absorption is approximately 50 meV.

Similar absorption spectra have been reported by Capizzi and Frova.[21,22] They argued that the 3.220 eV absorption edge originates from the band-to-band transition involving a 51 meV LO phonon absorption and the 3.271 eV absorption edge corresponds to defect-mediated transition. Since SrTiO$_3$ is an indirect gap semiconductor, the absorption and emission of momentum-conserving phonons at the zone boundary are needed during the light absorption and emission processes. However, Raman- and neutron-scattering studies show that a phonon with approximately 50 meV is observed only at the $k=0$ point; no phonons with approximately 50 meV are observed at the zone boundary.[23–25] On the other hand, the phonon energy of 25 meV is close to the transverse optical (TO$_2$) phonon energy at the zone boundary.[23,25] Then, we consider that optical transitions are assisted by the 25 meV phonon rather than 50 meV phonon. Two absorption edges (their energy separation: 50 meV) correspond to the band-to-band transitions involving phonon-absorption ($E_g-\hbar\omega_{ph}$) and emission ($E_g+\hbar\omega_{ph}$) processes with $\hbar\omega_{ph}=25$ meV, where E_g and $\hbar\omega_{ph}$ are the band-gap energy and phonon energy. The solid curves in Fig. 1(b) show the calculated absorption spectra by the theory of optical transition in indirect-gap semiconductors[26] for 85 and 8 K with the phonon energy of 25 meV. The good agreement of the experimental and theoretical results confirms that the low- and
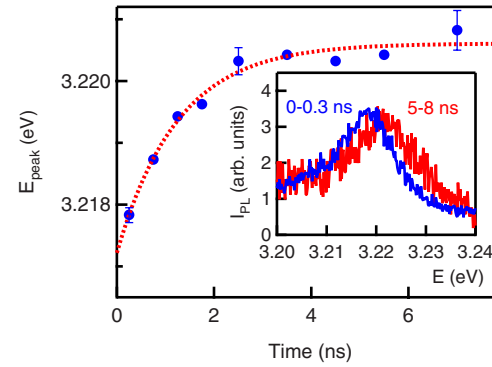
high-temperature onsets of the absorption spectra correspond to the 25 meV phonon-assisted transitions. Figure 1 also shows that the two PL peak energies coincide with the phonon-assisted optical transition energies. Thus, we can conclude that the PL peaks at 3.220 and 3.271 eV are band-to-band optical transitions (i.e., recombination of free electrons and holes) involving 25 meV phonon emission and absorption.

The band-edge PL of highly photoexcited SrTiO$_3$ is both time and excitation-density dependent. The inset of Fig. 2 shows the PL spectra gated at 0–0.3 ns and 5–8 ns. The time evolution of the peak energy of the lower energy PL peak is shown in Fig. 2. The peak energy is 3.217 eV just after the excitation and approaches 3.221 eV. This shift of the band-edge PL peak at the initial stage indicates band-gap shrinkage, which typically occurs in semiconductors under high-density photoexcitation due to the band-gap renormalization effect.[27] The temporal dependence of the PL peak energy reflects the photocarrier decay dynamics. Based on the above results, we determined the band-gap energy of undoped SrTiO$_3$ to be 3.246 eV.

To gain a deeper insight into the band-edge PL, we performed PL measurements in electron-doped SrTiO$_3$ under cw photoexcitation. Note that the photocarrier density under cw excitation is much smaller than that in pulse-laser excitation and the chemically doped electron density. Figure 3(a) shows the PL spectra of Nb-doped SrTiO$_3$ with various Nb concentrations at 8 K. As in the case of highly photoexcited SrTiO$_3$, two PL peaks are observed in all the samples with the exception of an anomalous PL peak at 3.21 eV in the 0.02 mol % Nb-doped SrTiO$_3$. The band-edge PL in the electron-doped samples corresponds to recombination of electrons that are present in the conduction band due to the doping and holes in the valence band due to photoexcitation. The charge-carrier density dependence of the PL spectral widths and peak energies is summarized in Fig. 3(b). The peak energy and spectral width of the two PL peaks show the same dependence on Nb concentration, suggesting that the two band-edge PL peaks have the same origin; phonon-assisted band-to-band radiative recombination. The spectral widths of the two PL peaks broaden with increasing carrier density. This broadening is attributed to alloy disorder in doped semiconductors.[27,28]
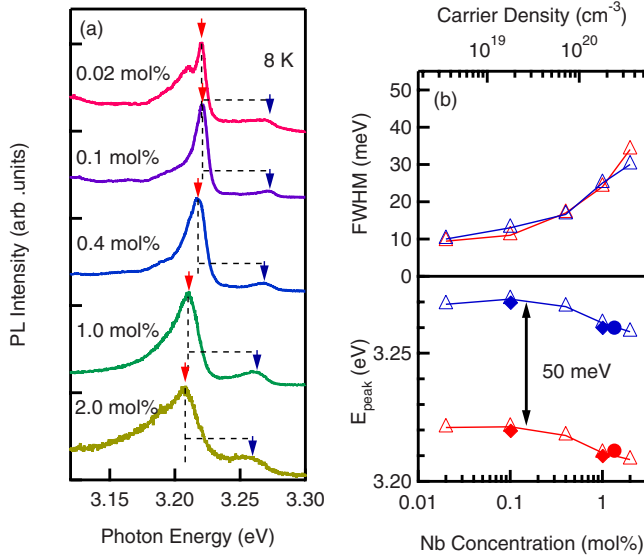

FIG. 2. (Color online) Time evolution of the peak energy of the lower band-edge PL peak of SrTiO$_3$ under excitation of 5 mJ/cm^2. The dotted curve is an eye guiding. The inset shows the PL spectra gated at 0–0.3 ns and 5–8 ns.

FIG. 3. (Color online) (a) PL spectra of Nb-doped SrTiO$_3$ with Nb concentration of 0.02, 0.1, 0.4, 1.0, and 2.0 mol % at 8 K. (b) Spectral width and peak energy of the band-edge PL in Nb-doped SrTiO$_3$ (△), La-doped SrTiO$_3$ (◆), and Ar$^+$-irradiated SrTiO$_3$ (●) as a function of the charge-carrier density.

The PL peaks redshift with increasing carrier density, and the separation of the two peaks (corresponding to two times the TO$_2$ phonon energy) is independent of the Nb concentration. This is consistent with a previous report that the TO$_2$ phonon energy is independent of the Nb concentration.[29] Band-edge PL was also observed in other electron-doped SrTiO$_3$ including La-doped SrTiO$_3$ and Ar$^+$-irradiated SrTiO$_3$. The peak energy of these electron-doped samples is plotted as a function of doped carrier density in Fig. 3(b), where the carrier density of the sample was estimated based on values reported in the literature[30] assuming a linear relationship between the carrier density and the dopant concentration. The electron density, N_e, in SrTi$_{1-x}$Nb$_x$O$_3$ is approximated by $N_e = 1.78 \times 10^{22} \times x$ cm^{-3}. The peak energy depends only on the carrier density, regardless of the dopant species, indicating that the carrier density determines the peak energy of band-edge PL. This result is consistent with the peak energy shift in highly photoexcited SrTiO$_3$, i.e., the band-gap shrinkage occurs owing to the high density of charge carriers.

We also measured the temperature dependence of the band-edge PL peaks. Figure 4 shows the PL spectra of SrNb$_{0.001}$Ti$_{0.999}$O$_3$ at 8, 20, 50, 75, and 100 K. The square root of the absorption coefficient is also plotted in the same figure. The solid curves for the absorption spectra show the theoretical curves with the phonon energy of 25 meV. The PL peak energies and spectral widths show the same temperature dependence. The PL peaks blueshift with increasing temperature and broaden. Above 100 K, the band-edge PL peaks become much broader and ill defined. The broadening of the high-energy tail at higher temperatures suggests a thermal distribution of carriers. In contrast to the PL peak energy, the onset of the linear dependence of $\alpha^{1/2}$ on energy is almost independent of temperature, indicating that the band-gap remains constant below 100 K.
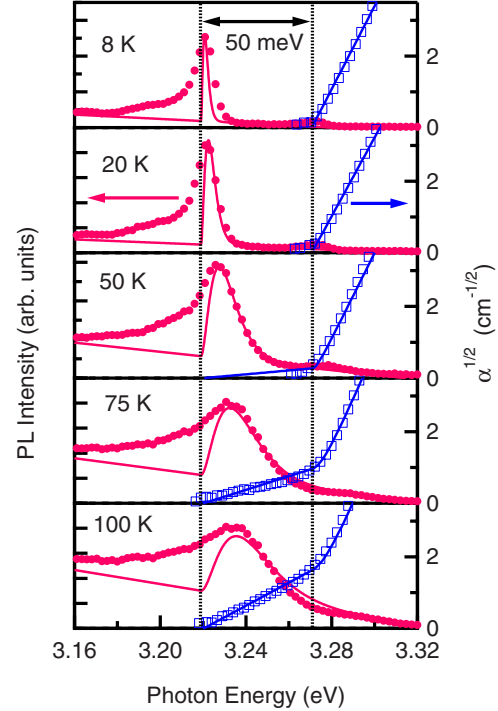

FIG. 4. (Color online) PL spectra (●) and the square root of the absorption coefficient (□) of SrNb$_{0.001}$Ti$_{0.999}$O$_3$ at 8, 20, 50, 75, and 100 K. The calculated band-to-band PL spectra using Eq. (1) and calculated optical absorption spectra with the phonon energy of 25 meV for indirect-gap semiconductors are shown as solid curves.

Here, we discuss the temperature dependence of the spectral shape of the band-to-band PL. According to Ref. 26, the spectral shape of band-to-band PL in indirect-gap semiconductors is described as

$$I_{PL}^\pm(\hbar\omega)$$
$$\propto (\hbar\omega - E_g \pm \hbar\omega_{ph})^2$$
$$\times \exp\left(-\frac{\hbar\omega - E_g \pm \hbar\omega_{ph}}{k_B T}\right) \quad (\text{for } \hbar\omega > E_g \mp \hbar\omega_{ph})$$
$$= 0 \quad (\text{otherwise}), \tag{1}$$

where the $\pm$ indicates (+) phonon emission and (−) phonon absorption. The solid curves in Fig. 4 are calculated results of band-to-band PL involving phonon-emission process using Eq. (1), where $E_g = 3.245$ eV and $\hbar\omega_{ph} = 25$ meV. We also included a linear background component, which results from the tail of the broad blue PL around 2.9 eV (see the inset of Fig. 1). The calculated curves reproduce the higher energy side of the band-edge PL above 20 K. Below the PL peak energy, we observed the low-energy tail, which is in poor agreement with the calculated curves. A similar low-energy tail is also observed in highly photoexcited undoped SrTiO$_3$ (see Fig. 1). This result suggests that very shallow localized states exist near the band edge. One possible origin of this localized state is a band-tail state caused by crystal disorder, which typically appears in mixed crystals, but could be present in undoped crystals. In addition, because SrTiO$_3$ has an indirect-gap and complicated band structure, we need

to consider optical transitions mediated by defects or impurities, as pointed out by Capizzi and Frova. As discussed above, however, the band-edge PL at 3.220 eV is well described in terms of phonon-assisted band-to-band transitions.

In conclusion, we found the band-to-band PL peaks in highly photoexcited $SrTiO_3$ and electron-doped $SrTiO_3$ at low temperatures. The two band-edge PL peaks correspond to radiative band-to-band recombination involving phonon emission and absorption processes. The band-edge PL peaks redshift with increasing carrier density, reflecting the band-gap shrinkage due to the band-gap renormalization effect. The observation of band-edge PL allows us an accurate determination of the band gap of $SrTiO_3$, which was found to be 3.246 eV. Band-to-band PL provides a powerful method for studying the electronic structure of bulk $SrTiO_3$ and $SrTiO_3$-based heterostructures.

*Corresponding author; kanemitu@scl.kyoto-u.ac.jp

[1] D. A. Muller, N. Nakagawa, A. Ohtomo, J. L. Grazul, and H. Y. Hwang, Nature (London) **430**, 657 (2004).
[2] Y. Muraoka, T. Muramatsu, J. Yamaura, and Z. Hiroi, Appl. Phys. Lett. **85**, 2950 (2004).
[3] H. P. R. Frederikse, W. R. Thurber, and W. R. Hosler, Phys. Rev. **134**, A442 (1964).
[4] O. N. Tufte and P. W. Chapman, Phys. Rev. **155**, 796 (1967).
[5] J. F. Schooley, W. R. Hosler, and M. L. Cohen, Phys. Rev. Lett. **12**, 474 (1964).
[6] H. Suzuki, H. Bando, Y. Ootuka, I. H. Inoue, T. Yamamoto, K. Takahashi, and Y. Nishihara, J. Phys. Soc. Jpn. **65**, 1529 (1996).
[7] J. Son, P. Moetakef, B. Jalan, O. Bierwagen, N. J. Wright, R. Engel-Herbert, and S. Stemmer, Nature Mater. **9**, 482 (2010).
[8] A. Ohtomo and H. Y. Hwang, Nature (London) **427**, 423 (2004).
[9] G. Herranz, M. Basletic, M. Bibes, C. Carrétéro, E. Tafra, E. Jacquet, K. Bouzehouane, C. Deranlot, A. Hamzić, J. M. Broto, A. Barthélémy, and A. Fert, Phys. Rev. Lett. **98**, 216803 (2007).
[10] Y. Kozuka, M. Kim, C. Bell, B. G. Kim, Y. Hikita, and H. Y. Hwang, Nature (London) **462**, 487 (2009).
[11] J. Mannhart and D. G. Schlom, Science **327**, 1607 (2010).
[12] K. Ueno, S. Nakamura, H. Shimotani, A. Ohtomo, N. Kimura, T. Nojima, H. Aoki, Y. Iwasa, and M. Kawasaki, Nature Mater. **7**, 855 (2008).
[13] T. Feng, Phys. Rev. B **25**, 627 (1982).
[14] R. Leonelli and J. L. Brebner, Phys. Rev. B **33**, 8649 (1986).
[15] T. Hasegawa, M. Shirai, and K. Tanaka, J. Lumin. **87-89**, 1217 (2000).
[16] D. Kan, T. Terashima, R. Kannda, A. Masuno, K. Tanaka, S. Chu, H. Kan, A. Ishizumi, Y. Kanemitsu, Y. Shimakawa, and M. Takano, Nature Mater. **4**, 816 (2005).
[17] H. Yasuda and Y. Kanemitsu, Phys. Rev. B **77**, 193202 (2008).
[18] Y. Yamada, H. Yasuda, T. Tayagaki, and Y. Kanemitsu, Phys. Rev. Lett. **102**, 247401 (2009).
[19] Y. Yamada, H. Yasuda, T. Tayagaki, and Y. Kanemitsu, Appl. Phys. Lett. **95**, 121112 (2009).
[20] A. Rubano, D. Paparo, F. Miletto, U. Scotti di Uccio, and L. Marrucci, Phys. Rev. B **76**, 125115 (2007).
[21] M. Capizzi and A. Frova, Phys. Rev. Lett. **25**, 1298 (1970).
[22] A. Frova, Nuovo Cimento B **55**, 1 (1968).
[23] C. H. Perry, J. H. Fertel, and T. F. McNelly, J. Chem. Phys. **47**, 1619 (1967).
[24] R. F. Schaufele and M. J. Weber, J. Chem. Phys. **46**, 2859 (1967).
[25] W. G. Nilsen and J. G. Skinner, J. Chem. Phys. **48**, 2240 (1968).
[26] P. Y. Yu and M. Cardona, *Fundamentals of Semiconductors*, 3rd ed. (Springer, Berlin, 2005).
[27] C. F. Klingshirn, *Semiconductor Optics*, 3rd ed. (Springer, Berlin, 2007).
[28] R. Zimmermann, J. Cryst. Growth **101**, 346 (1990).
[29] F. Gervais, J.-L. Servoin, A. Baratoff, J. G. Bednorz, and G. Binnig, Phys. Rev. B **47**, 8187 (1993).
[30] S. Ohta, T. Nomura, H. Ohta, and K. Koumoto, J. Appl. Phys. **97**, 034106 (2005).